Letter

Radiative lifetime of the $A\ ^2\Pi_{1/2}$ state in RaF with relevance to laser cooling

M. Athanasakis-Kaklamanakis,[1,2,3,*] S. G. Wilkins,[4,5] P. Lassègues,[2] L. Lalanne,[1] J. R. Reilly,[6] O. Ahmad,[2] M. Au,[7,8] S. W. Bai,[9] J. Berbalk,[2] C. Bernerd,[7] A. Borschevsky,[10] A. A. Breier,[11,12] K. Chrysalidis,[7] T. E. Cocolios,[2] R. P. de Groote,[2] C. M. Fajardo-Zambrano,[2] K. T. Flanagan,[6,13] S. Franchoo,[14] R. F. Garcia Ruiz,[4,5] D. Hanstorp,[15] R. Heinke,[7] P. Imgram,[2] Á. Koszorús,[1,2] A. A. Kyuberis,[10] J. Lim,[3] Y. C. Liu,[9] K. M. Lynch,[6] A. McGlone,[6] W. C. Mei,[9] G. Neyens,[2,†] L. Nies,[1] A. V. Oleynichenko,[16] A. Raggio,[17] S. Rothe,[7] L. V. Skripnikov,[16] E. Smets,[2] B. van den Borne,[2] J. Warbinek,[18,19] J. Wessolek,[6,7] and X. F. Yang[9]

[1]*Experimental Physics Department, CERN, CH-1211 Geneva 23, Switzerland*
[2]*KU Leuven, Instituut voor Kern- en Stralingsfysica, B-3001 Leuven, Belgium*
[3]*Centre for Cold Matter, Imperial College London, London SW7 2AZ, United Kingdom*
[4]*Department of Physics, Massachusetts Institute of Technology, Cambridge, Massachusetts 02139, USA*
[5]*Laboratory for Nuclear Science, Massachusetts Institute of Technology, Cambridge, Massachusetts 02139, USA*
[6]*Department of Physics and Astronomy, The University of Manchester, Manchester M13 9PL, United Kingdom*
[7]*Systems Department, CERN, CH-1211 Geneva 23, Switzerland*
[8]*Department of Chemistry, Johannes Gutenberg-Universität Mainz, D-55128 Mainz, Germany*
[9]*School of Physics and State Key Laboratory of Nuclear Physics and Technology, Peking University, Beijing 100971, China*
[10]*Van Swinderen Institute of Particle Physics and Gravity, University of Groningen, NL-9747 CP Groningen, Netherlands*
[11]*Institut für Optik und Atomare Physik, Technische Universität Berlin, D-10623 Berlin, Germany*
[12]*Laboratory for Astrophysics, Institute of Physics, University of Kassel, D-34132 Kassel, Germany*
[13]*Photon Science Institute, The University of Manchester, Manchester M13 9PY, United Kingdom*
[14]*Laboratoire Irène Joliot-Curie, CNRS/IN2P3 and University Paris-Saclay, 91405 Orsay, France*
[15]*Department of Physics, University of Gothenburg, SE-41296 Gothenburg, Sweden*
[16]*Affiliated with an institute covered by a cooperation agreement with CERN*
[17]*Department of Physics, University of Jyväskylä, FI-40014 Jyväskylä, Finland*
[18]*GSI Helmholtzzentrum für Schwerionenforschung GmbH, D-64291 Darmstadt, Germany*
[19]*Department of Chemistry - TRIGA Site, Johannes Gutenberg-Universität Mainz, D-55128 Mainz, Germany*

(Received 14 March 2024; accepted 31 May 2024; published 22 July 2024)

The radiative lifetime of the $A\ ^2\Pi_{1/2}$ $(v = 0)$ state in radium monofluoride (RaF) is measured to be 35(1) ns. The lifetime of this state and the related decay rate $\Gamma = 2.86(8) \times 10^7\ \mathrm{s}^{-1}$ are of relevance to the laser cooling of RaF via the optically closed $A\ ^2\Pi_{1/2} \leftarrow X\ ^2\Sigma_{1/2}$ transition, which makes the molecule a promising probe to search for new physics. RaF is found to have a comparable photon-scattering rate to homoelectronic laser-coolable molecules. Owing to its highly diagonal Franck-Condon matrix, it is expected to scatter an order of magnitude more photons than other molecules when using just three cooling lasers, before it decays to a dark state. The lifetime measurement in RaF is benchmarked by measuring the lifetime of the $8P_{3/2}$ state in Fr to be 83(3) ns, in agreement with literature.

DOI: 10.1103/PhysRevA.110.L010802

Introduction. The properties of the lowest-lying $^2\Pi_{1/2}$ state in alkaline-earth-metal monofluorides and other homoelectronic molecules are of central importance for their suitability for direct laser cooling and trapping. The diagonal Franck-Condon matrix and closed optical cycle between the $X\ ^2\Sigma^+$ ground state and the lowest-lying $A\ ^2\Pi_{1/2}$ state of these molecules has enabled the direct laser cooling of molecules to mK temperatures or lower, such as CaF [1], SrF [2], YbF [3], YO [4], CaOH [5], SrOH [6], and the symmetric-top $CaOCH_3$ [7]. The short radiative lifetime of the $A\ ^2\Pi_{1/2}$ state is key for efficient laser cooling based on the optically closed $A\ ^2\Pi_{1/2} \leftarrow X\ ^2\Sigma^+$ transition, and decelerating the molecules to the capture velocity of a magneto-optical trap [8].

The homoelectronic and radioactive RaF has been proposed as a sensitive probe for searches of parity or time-reversal (P, T) violating properties, such as the electric dipole moment of the electron (eEDM). Extending laser cooling and trapping to RaF would enable highly sensitive searches for new physics by significantly increasing the interrogation time of the RaF molecules.

*Contact author: m.athkak@cern.ch
†Contact author: gerda.neyens@kuleuven.be

Owing to the high atomic number of Ra ($Z = 88$), the ground state of RaF, whose longest-lived isotopologue ^{226}Ra ^{19}F has a half-life of 1600 years, is highly sensitive to the eEDM [9,10]. Furthermore, the octupole-deformed shape of the $^{222-226}$Ra nuclei [11] also enhances the sensitivity of RaF to a number of P, T-violating nuclear properties [12], such as the Schiff moment [9,13]. Combined with the potential to achieve exceptionally long coherence times owing to laser cooling, RaF is a promising system to search for new physics with potentially unprecedented sensitivity.

To determine the maximum photon scattering rate and the required interaction time for laser slowing of RaF, knowledge of the radiative lifetime of the upper state in the closed optical cycle is necessary. This Letter presents the experimental measurement of the radiative lifetime of the $A\ ^2\Pi_{1/2}$ state in RaF at 35(1) ns, via delayed multistep ionization using broadband pulsed lasers (> 3 GHz). Prior to this work, only an upper limit of $\tau < 50$ ns was reported for this state [14]. The result is benchmarked by applying the same measurement procedure also for the $8P_{3/2}$ state of neutral Fr, for which a lifetime value was previously reported and lies in the same order of magnitude as that for $A\ ^2\Pi_{1/2}$ in RaF. The benchmark measurement of 83(3) ns in this study is consistent with the literature value of 83.5(15) ns [15] within 1σ.

Methods. The measurements were obtained via delayed multistep ionization with the collinear resonance ionization spectroscopy (CRIS) experiment using beams of ^{226}Ra ^{19}F$^+$ and ^{221}Fr$^+$ produced at the ISOLDE radioactive ion beam facility at CERN. The technique and the employed laser schemes are shown schematically in Fig. 1, and further experimental details can be found in the Supplemental Material [16] and in Refs. [17–19].

Fast ions (∼40 keV kinetic energy) of ^{226}Ra ^{19}F$^+$ and ^{221}Fr$^+$, released as a pulsed beam from a linear Paul trap (100-Hz repetition, 5-μs temporal spread, 0.8-m longitudinal spatial spread), were delivered to the CRIS experiment and were neutralized via collisions with a vapor of sodium atoms in a charge-exchange cell, while the remaining ions were deflected onto a beam dump. The neutralized bunches entered the interaction region, where they were temporally and spatially overlapped in a collinear geometry with pulsed laser beams [see Fig. 1(a)] that stepwise excited the molecules/atoms from the ground state to above the ionization potential, as per the laser schemes shown in Figs. 1(b) and 1(c). The resonantly reionized molecules were deflected onto a MagneTOF single-ion detector, while the residual neutral beam was discarded onto a beam dump.

All lasers in this study were pulsed and broadband, with linewidths $\Delta f \geqslant 3$ GHz. The 753-nm step in RaF was produced with the fundamental output of a Ti:sapphire laser, while the 423-nm excitation step in Fr was produced by second-harmonic generation of the same Ti:sapphire laser. The 646-nm step in RaF was produced using a dye laser pumped by a 532-nm Nd:YAG laser. The 532- and 1064-nm steps were produced by the second and fundamental harmonics of a Nd:YAG laser, respectively. The 646- and 532-nm steps in RaF and 1064-nm step in Fr are referred to as the ionization steps, while the 753- and 423-nm steps are referred to as the excitation steps in the respective schemes in this Letter.

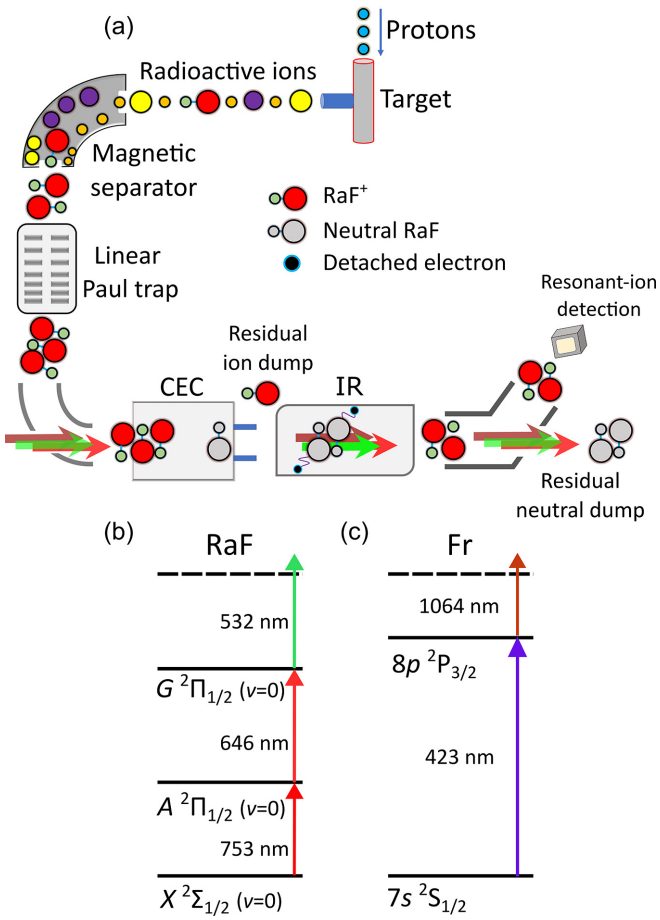

FIG. 1. Top: (a) Summary of the experimental setup, showing the production, mass separation, bunching in a Paul trap, neutralization in the charge-exchange cell (CEC), and resonant ionization in the interaction region (IR). Bottom: Laser excitation scheme used for (b) RaF and (c) Fr in this work, denoting the rest-frame transition wavelengths.

The pulses of the laser used for the excitation steps had a full width at half maximum (FWHM) of 38(2) ns, while the pulses of the Nd:YAG lasers used for the ionization steps had a FWHM of 15(1) ns. The shot-to-shot jitter of the excitation step was measured to be 4 ns and that of the ionization steps to be 3 ns, for a total relative shot-to-shot jitter of 5 ns (added in quadrature) between excitation and ionization steps in both schemes (details in the Supplemental Material [16]). As the 646-nm step in the RaF scheme was provided by a pulsed dye laser pumped by an identical Nd:YAG laser as the one used for the 532-nm ionization step, the FWHM and jitter of the second and third steps were measured to be the same, as expected.

To determine the lifetime of the $A\ ^2\Pi_{1/2}$ state in RaF and the $8P_{3/2}$ state in Fr, multiple measurement cycles were performed for various timing arrangements between the ejection of the molecular/atomic beam from the gas-filled linear Paul trap of the ISOLDE facility [20] and the timing of the laser pulses. First, an optimal setting for the Paul trap ejection timing was determined based on the maximum laser-molecule/atom spatial and temporal overlap, and a lifetime measurement was taken for these settings, by moving the

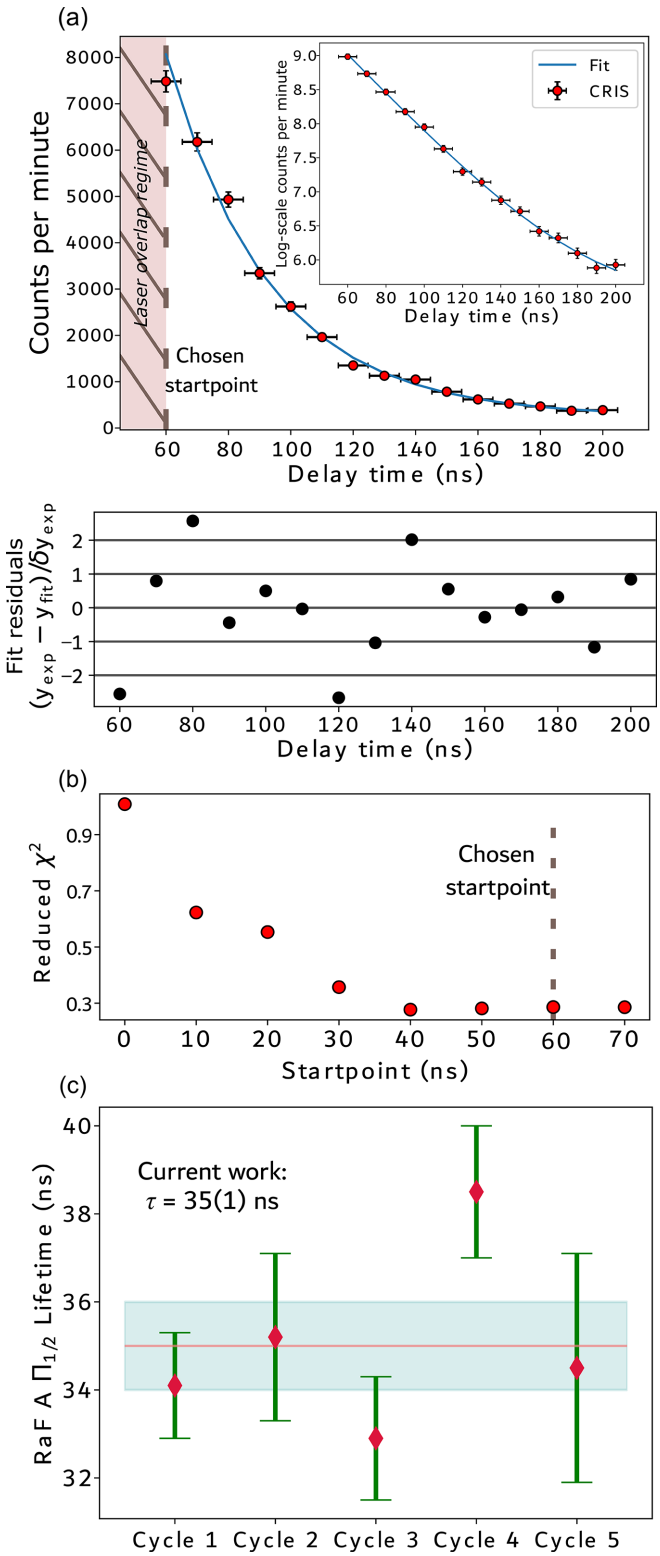

FIG. 2. (a) Example decay curve (top) and fit residuals (bottom) for a single measurement cycle in RaF. The y errors include both statistical and systematic components, and the x error, the same for all points, corresponds to the total relative jitter of the lasers (see text and Supplemental Material [16] for details). The inset shows the same plot with the y axis in logarithmic scale. (b) Example curve of reduced χ^2 as a function of the fit start point in the data subset of the full decay curve for a single measurement cycle in RaF, used to confirm the start of free radiative decay (see text for details). (c) Extracted lifetime values for individual measurement cycles in RaF. The line and surrounding band denote the error-weighted mean and its standard deviation across all five measurement cycles, respectively.

timing of the ionization steps forward in time while keeping the timing of the excitation step fixed. Lifetime measurements (denoted as cycle 1 for both RaF and Fr) were performed for this optimal ejection timing, as well as for ejection timings 0.5 μs earlier and 0.5 μs later compared to the optimal for Fr (1-μs steps for RaF). One lifetime measurement was also performed at the optimal ejection timing, but moving the excitation step timing backwards while keeping the timing of the ionization steps fixed. Only for the RaF experiment, an additional measurement [cycle 4 in Fig. 2(c)] had been performed in a separate proof-of-principle experimental campaign 2 years prior to the rest of the cycles; details about this measurement cycle can be found in the Supplemental Material [16].

Figure 2(a) shows an example of the measured ion count rate as a function of the delay time t between the excitation step and the subsequent ionization steps (all decay curves are shown in the Supplemental Material [16]). For delay times larger than the sum of the pulse widths (FWHM) and the relative jitter, the data represent the radiative decay from the excited $A\,^2\Pi_{1/2}$ state, and the curve can then be fitted with the natural decay law:

$$N(t) = N_0 e^{-t/\tau} + C. \tag{1}$$

In Eq. (1), $N(t)$ is the population of molecules in the $A\,^2\Pi_{1/2}$ state as a function of the delay, N_0 is the population at delay time $t = 0$, τ is the radiative lifetime of the $A\,^2\Pi_{1/2}$ state, and C is a constant representing the ion background on the detector that stems from nonresonant ionization. In order to exclude data points where the radiative decay law is not valid (at times when there is an overlap of the lasers), the first 60 ns were omitted when fitting the decay curve, shown as the "laser overlap regime" in Fig. 2(a). This span of 60 ns is approximately equal to the sum of the FWHM and relative jitter of the lasers (see Supplemental Material [16] for details).

The laser overlap regime was confirmed as shown in Fig. 2(b), where the delay time at which the reduced χ^2 saturates is verified, which marks the end of the laser overlap regime. While saturation already start from 40 ns, all decay curves were analyzed with a 60-ns start point to exclude data with partial laser overlap. Fitting the decay curves with start points between 40 and 70 ns resulted in consistent lifetime values. The same procedure was followed for Fr.

A 5-ns error was adopted for the laser delay time, which corresponds to the combined shot-to-shot laser jitter of the excitation and ionization lasers (see Supplemental Material [16]). Repeating the fit procedure with a smaller x error yielded a reduced χ^2 progressively closer to 1, while the lifetime result remained unchanged. The uncertainties on the final lifetime values were not scaled with the respective reduced χ of each fit, as this would reduce the uncertainty, and it is preferred to remain conservative in the result.

The fit residuals for the decay curve are shown in Fig. 2(a). The fraction of data points whose deviation from the fit ex-

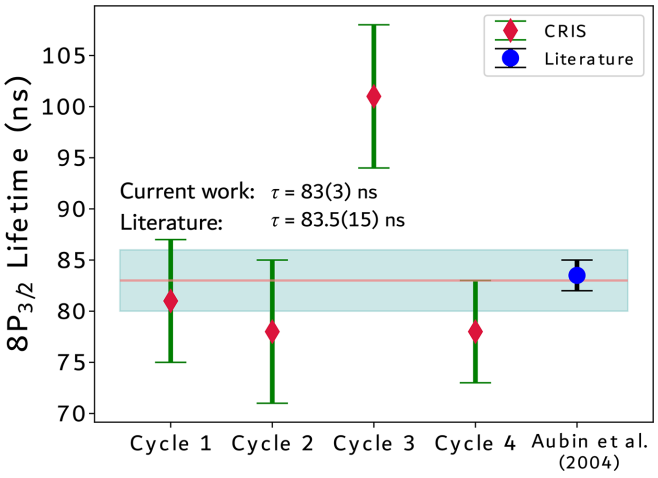

FIG. 3. Lifetime results for the $8P_{3/2}$ state in Fr as a benchmark study. The central line and surrounding band represent the error-weighted mean and one standard deviation of the lifetime values of the individual measurement cycles. The final result of 83(3) ns in this benchmark study is in agreement with the literature value from Ref. [15].

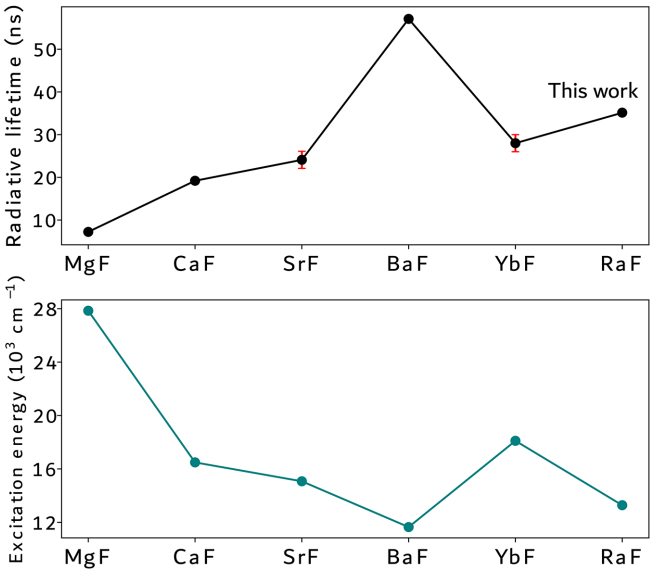

FIG. 4. Comparison of the radiative lifetime (upper) and excitation energy (lower) of the $A\ ^2\Pi_{1/2}$ state in RaF with MgF [21], CaF [22,23], SrF [24,25], BaF [26,27], and YbF [28,29]. In most cases, the error bar is smaller than the data marker.

ceeds the y error is consistent with the 1σ confidence interval. A potential oscillatory trend in the residuals, not seen in all data sets (see Fig. 4 in Supplemental Material [16]), falls within the confidence interval.

In Fig. 2(c), the final results from the lifetime analysis for RaF are presented, extracted from the different measurement cycles that cover different experimental conditions. The weighted mean value of the independent measurements is found to be 35(1) ns.

To test the accuracy of the experimental approach and analysis procedure, the lifetime of the $8P_{3/2}$ state in Fr was measured using the same approach, and compared with a literature value from Aubin *et al.* [15]. The results are presented in Fig. 3, leading to a weighted mean value of 83(3) ns, consistent with the literature value of 83.5(15) ns [15].

Results and discussion. The lifetime of the $A\ ^2\Pi_{1/2}$ state in RaF was measured to be $\tau = 35(1)$ ns. The radiative lifetime and excitation energy of the $A\ ^2\Pi_{1/2}$ $(v = 0)$ states across alkaline-earth-metal monofluorides (and the homoelectronic YbF) are shown in Fig. 4. A trend of gradually increasing lifetime for increasing molecular mass is evident, which appears correlated with a decrease in the excitation energy of the $A\ ^2\Pi_{1/2}$ states.

The excitation energy is of importance for the laser-cooling scheme, as it determines the single-photon recoil velocity, $\hbar k/m$, where m is the mass of the molecule, $k = \frac{2\pi}{\lambda}$, and λ is the transition wavelength. The trends in Fig. 4 imply that laser-cooling efficiency decreases for heavier alkaline-earth-metal monofluorides, as the molecular mass and transition wavelength increase, while the increasing lifetime of the upper state leads to a reduced photon scattering rate. For the laser-cooling transition in RaF, the recoil velocity is equal to 0.22 cm s^{-1}.

Based on the lifetime $\tau = 35(1)$ ns, the radiative decay rate $\Gamma = \frac{1}{\tau} = 2.86(8) \times 10^7$ s^{-1} can be extracted. Γ is a key quantity for a number of spectroscopic properties, such as the natural linewidth $(\Gamma/2\pi)$ of the $A\ ^2\Pi_{1/2} \leftarrow X\ ^2\Sigma_{1/2}$ transition, which is found to be equal to 4.6(1) MHz, and the maximum photon scattering rate $R_{\rm sc}^{\rm max}$ of the transition.

For the laser-cooling scheme proposed in Ref. [30], $R_{\rm sc}^{\rm max}$ can be approximated for optimistic conditions of a magneto-optical trap as $R_{\rm sc}^{\rm max} = \Gamma/7$, based on a set of rate equations as summarized in Ref. [31], which in this case is equal to $R_{\rm sc}^{\rm max} = 4.1(1) \times 10^6$ s^{-1}. With this scattering rate, the optically closed $A\ ^2\Pi_{1/2} \leftarrow X\ ^2\Sigma_{1/2}$ transition in RaF could scatter 100 000 photons in 24.4(7) ms, assuming identical Γ for the $v = 0, 1, 2$ states of $A\ ^2\Pi_{1/2}$ [30]. It is noted that the accuracy of this expression for $R_{\rm sc}^{\rm max}$ is limited by the validity of the rate model in a practical setting [31], and these results thus represent optimistic values. It is possible that experimental measurements of the scattering rate could be lower than this value.

Lastly, considering the photon recoil velocity of 0.22 cm s^{-1}, the maximum scattering rate implies a photon scattering acceleration of $a_\gamma = R_{\rm sc}^{\rm max}\hbar k/m = 9.0(3)$ km s^{-2}. These results are summarized in Table I.

Figure 5 compares, based on the lifetime of the $A\ ^2\Pi_{1/2}$ state and the Franck-Condon factors, the expected performance of laser cooling for RaF and stable diatomic molecules

TABLE I. Summary of present results on the radiative decay of the $A\ ^2\Pi_{1/2}$ $(v = 0)$ state in RaF.

Radiative lifetime τ (ns)	35(1)
Radiative decay rate Γ (s^{-1})	$2.86(8) \times 10^7$
Maximum scattering rate $R_{\rm sc}^{\rm max}$ (s^{-1})	$4.1(1) \times 10^6$
Natural linewidth $\Gamma/2\pi$ (MHz)	4.6(1)
Recoil velocity $\hbar k/m$ (cm s^{-1})	0.22
Doppler limit $\hbar\Gamma/2k_B$ (μK)	109(3)
Scattering acceleration a_γ (km s^{-2})	9.0(3)

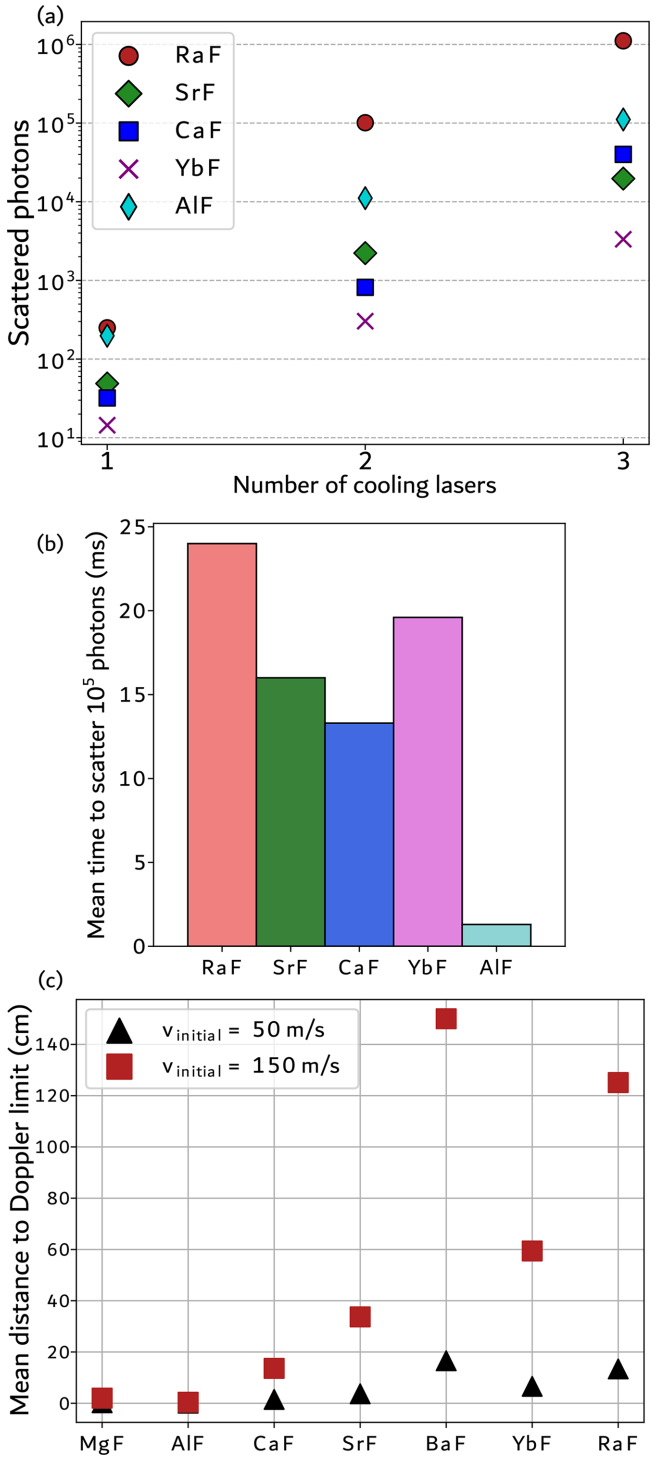

FIG. 5. (a) Comparison of number of photons that can be scattered using the $A\,\Pi$-$X\,\Sigma$ transition before RaF, SrF, CaF, YbF, and AlF molecules would land in a dark state as a function of the number of cooling lasers. It is noted that laser cooling in AlF is based on the $A\,^1\Pi - X\,^1\Sigma$ transition, contrary to the $A\,^2\Pi - X\,^2\Sigma$ transition for the other molecules. (b) Average time to scatter 10^5 photons for the same molecules using the $A\Pi - X\,\Sigma$ laser-cooling cycle. Values were extracted using reported Franck-Condon factors and radiative decay rates [2,3,30,32,33], and the current result for the lifetime of $A\,^2\Pi_{1/2}$ in RaF. (c) Comparison of mean distance required to slow to the Doppler limit a molecular beam produced by a cryogenic buffer-gas cell.

that have been successfully cooled, all featuring a laser-cooling cycle based on optically closed $\Sigma - \Pi$ transitions. Due to its highly diagonal Franck-Condon matrix for the $A\,\Pi - X\,\Sigma$ transition [30], which far exceeds the diagonality of the transition in the other molecules, the $A\,^2\Pi_{1/2} - X\,^2\Sigma_{1/2}$ transition in RaF can scatter an order of magnitude more photons when using three cooling lasers before a significant fraction of the molecules is lost to higher vibrational states, while potentially scattering up to 10^5 photons using only two lasers that address the $v = 0, 1$ vibrational states, as shown in Fig. 5(a).

Although the radiative decay rate Γ is the smallest for RaF, the time required to scatter 10^5 photons, which can also serve as a measure of the time required to slow a molecular beam down to the capture velocity of a magneto-optical trap, is comparable to that for other molecules [Fig. 5(b)]. Molecular beams produced by cryogenic buffer-gas cells, which most often serve as the source in molecular trapping setups, are emitted with forward velocities that appear to be weakly dependent on the molecular mass of the beam [34,35]. Figure 5(c) compares the distance required to slow a molecular beam down to the Doppler limit using counterpropagating laser cooling. For a forward velocity of 50 m/s, which is achievable with a two-stage buffer-gas cell at 1 K, the difference in slowing RaF compared to the lighter molecules becomes insignificant for a beamline of realistic dimensions.

As a result, the diagonality of the transition in RaF, which could allow effective laser cooling with fewer lasers, is accompanied by a scattering rate that is comparable to that of other laser-cooled molecules. A more conclusive discussion on the number of photons scattered by RaF per cooling laser would require direct measurements of vibrational branching ratios in the future.

Beyond RaF, other radium-containing molecules have also been proposed for searches of new physics based on calculations of a laser-coolable electronic structure. Neutral polyatomic radium-containing molecules appear to have lifetimes in the ns range, such as $\tau_{\text{calc}} = 40$ ns for RaOH [36], making them similarly promising candidates as RaF for laser cooling and trapping. Therefore, experimental methods for the measurement of symmetry-violating moments based on laser-slowed and laser-cooled neutral molecules [37] are expected to be critical for progress in designing sensitive searches for new physics with radium-containing molecules.

Conclusions. In this Letter, the measurement of the radiative lifetime of the $A\,^2\Pi_{1/2}$ ($v = 0$) state in RaF is presented. The lifetime was measured via delayed multistep ionization using the CRIS experiment at the CERN-ISOLDE radioactive ion beam facility. The lifetime is determined to be $\tau = 35(1)$ ns. Using this value, the radiative decay rate $\Gamma = 2.86(8) \times 10^7\ \text{s}^{-1}$ is extracted, which further determines the maximum photon scattering rate $R_{\text{sc}}^{\text{max}} = 4.1(1) \times 10^6\ \text{s}^{-1}$. The validity of the lifetime measurement in RaF is benchmarked via a measurement of the lifetime of the $8P_{3/2}$ state in Fr using the same technique. The extracted lifetime for the $8P_{3/2}$ state in Fr at 83(3) ns in this work is in agreement with the literature value.

The quantities reported in this Letter are of direct relevance to simulations for efficient laser cooling of RaF. Laser-cooled and trapped neutral molecules are envisioned as sensitive

probes for future searches of new physics, and owing to its exceptionally diagonal Franck-Condon matrix, RaF is expected to scatter 10^5 photons using only two cooling lasers, while using three cooling lasers allows scattering an order of magnitude more photons than other laser-cooled molecules. While the photon-scattering acceleration is lower in RaF compared to the lighter homoelectronic molecules, it is shown that the difference becomes insignificant for a molecular source that produces a sufficiently slow beam (∼50 m/s).

Acknowledgments. We thank the ISOLDE technical teams for their support. This project has received funding from the European Union's Horizon Europe Research and Innovation programme EUROLABS under Grant Agreement No. 101057511 and the European Union's Horizon 2020 research and innovation programme under Grant Agreement No. 654002. Financial support from FWO, as well as from the Excellence of Science (EOS) programme (No. 40007501) and the KU Leuven Project No. C14/22/104, is acknowledged. The STFC consolidated Grants No. ST/V001116/1 and No. ST/P004423/1 and the FNPMLS ERC Grant Agreement No. 648381 are acknowledged. S.G.W. and R.F.G.R. acknowledge funding by the Office of Nuclear Physics, US Department of Energy Grants No. DE-SC0021176 and No. DE-SC002117. M. Au, A.R., J.Wa., and J.We. acknowledge funding from the EU's H2020-MSCA-ITN Grant No. 861198 "LISA." D.H. acknowledges financial support from the Swedish Research Council (2020-03505). J.L. acknowledges financial support from STFC Grant No. ST/V00428X/1. S.W.B., Y.C.L., W.C.M., and X.F.Y. acknowledge support from the National Natural Science Foundation of China (No. 12350007).

[1] V. Zhelyazkova, A. Cournol, T. E. Wall, A. Matsushima, J. J. Hudson, E. A. Hinds, M. R. Tarbutt, and B. E. Sauer, Laser cooling and slowing of CaF molecules, Phys. Rev. A **89**, 053416 (2014).

[2] E. S. Shuman, J. F. Barry, and D. DeMille, Laser cooling of a diatomic molecule, Nature (London) **467**, 820 (2010).

[3] J. Lim, J. R. Almond, M. A. Trigatzis, J. A. Devlin, N. J. Fitch, B. E. Sauer, M. R. Tarbutt, and E. A. Hinds, Laser cooled YbF molecules for measuring the electron's electric dipole moment, Phys. Rev. Lett. **120**, 123201 (2018).

[4] S. Ding, Y. Wu, I. A. Finneran, J. J. Burau, and J. Ye, Sub-Doppler cooling and compressed trapping of YO molecules at μK temperatures, Phys. Rev. X **10**, 021049 (2020).

[5] N. B. Vilas, C. Hallas, L. Anderegg, P. Robichaud, A. Winnicki, D. Mitra, and J. M. Doyle, Magneto-optical trapping and sub-Doppler cooling of a polyatomic molecule, Nature (London) **606**, 70 (2022).

[6] I. Kozyryev, L. Baum, K. Matsuda, B. L. Augenbraun, L. Anderegg, A. P. Sedlack, and J. M. Doyle, Sisyphus laser cooling of a polyatomic molecule, Phys. Rev. Lett. **118**, 173201 (2017).

[7] D. Mitra, N. B. Vilas, C. Hallas, L. Anderegg, B. L. Augenbraun, L. Baum, C. Miller, S. Raval, and J. M. Doyle, Direct laser cooling of a symmetric top molecule, Science **369**, 1366 LP (2020).

[8] M. R. Tarbutt, Laser cooling of molecules, Contemp. Phys. **59**, 356 (2018).

[9] T. A. Isaev, S. Hoekstra, and R. Berger, Laser-cooled RaF as a promising candidate to measure molecular parity violation, Phys. Rev. A **82**, 052521 (2010).

[10] S. G. Wilkins, S. M. Udrescu, M. Athanasakis-Kaklamanakis, R. F. G. Ruiz, M. Au, I. Belošević, R. Berger, M. L. Bissell, A. A. Breier, A. J. Brinson, K. Chrysalidis, T. E. Cocolios, R. P. de Groote, A. Dorne, K. T. Flanagan, S. Franchoo, K. Gaul, S. Geldhof, T. F. Giesen, D. Hanstorp *et al.*, Observation of the distribution of nuclear magnetization in a molecule, arXiv:2311.04121.

[11] P. A. Butler, L. P. Gaffney, P. Spagnoletti, K. Abrahams, M. Bowry, J. Cederkäll, G. de Angelis, H. De Witte, P. E. Garrett, A. Goldkuhle, C. Henrich, A. Illana, K. Johnston, D. T. Joss, J. M. Keatings, N. A. Kelly, M. Komorowska, J. Konki, T. Kröll, M. Lozano *et al.*, Evolution of octupole deformation in radium nuclei from Coulomb excitation of radioactive ^{222}Ra and ^{228}Ra beams, Phys. Rev. Lett. **124**, 042503 (2020).

[12] M. S. Safronova, D. Budker, D. DeMille, D. F. Jackson Kimball, A. Derevianko, and C. W. Clark, Search for new physics with atoms and molecules, Rev. Mod. Phys. **90**, 025008 (2018).

[13] A. D. Kudashov, A. N. Petrov, L. V. Skripnikov, N. S. Mosyagin, T. A. Isaev, R. Berger, and A. V. Titov, *Ab initio* study of radium monofluoride (RaF) as a candidate to search for parity- and time-and-parity-violation effects, Phys. Rev. A **90**, 052513 (2014).

[14] R. F. Garcia Ruiz, R. Berger, J. Billowes, C. L. Binnersley, M. L. Bissell, A. A. Breier, A. J. Brinson, K. Crysalidis, T. E. Cocolios, B. S. Cooper, K. T. Flanagan, T. F. Giesen, R. P. de Groote, S. Franchoo, F. P. Gustafsson, T. A. Isaev, A. Koszorus, G. Neyens, H. A. Perrett, C. M. Ricketts *et al.*, Spectroscopy of short-lived radioactive molecules, Nature (London) **581**, 396 (2020).

[15] S. Aubin, E. Gomez, L. A. Orozco, and G. D. Sprouse, Lifetimes of the 9*s* and 8*p* levels of atomic francium, Phys. Rev. A **70**, 042504 (2004).

[16] See Supplemental Material at http://link.aps.org/supplemental/10.1103/PhysRevA.110.L010802 for additional information on the experiment, data analysis, and complete results.

[17] R. Catherall, W. Andreazza, M. Breitenfeldt, A. Dorsival, G. J. Focker, T. P. Gharsa, T. J. Giles, J.-L. Grenard, F. Locci, P. Martins, S. Marzari, J. Schipper, A. Shornikov, and T. Stora, The ISOLDE facility, J. Phys. G: Nucl. Part. Phys. **44**, 094002 (2017).

[18] T. E. Cocolios, H. H. Al Suradi, J. Billowes, I. Budinčević, R. P. de Groote, S. De Schepper, V. N. Fedosseev, K. T. Flanagan, S. Franchoo, R. F. Garcia Ruiz, H. Heylen, F. Le Blanc, K. M. Lynch, B. A. Marsh, P. J. R. Mason, G. Neyens, J. Papuga, T. J. Procter, M. M. Rajabali, R. E. Rossel *et al.*, The collinear resonance ionization spectroscopy (CRIS) experimental setup at CERN-ISOLDE, Nucl. Instrum. Methods Phys. Res. Sect. B **317**, 565 (2013).

[19] M. Au, M. Athanasakis-Kaklamanakis, L. Nies, J. Ballof, R. Berger, K. Chrysalidis, P. Fischer, R. Heinke, J. Johnson, U.

Köster, D. Leimbach, B. Marsh, M. Mougeot, B. Reich, J. Reilly, E. Reis, M. Schlaich, C. Schweiger, L. Schweikhard, S. Stegemann *et al.*, In-source and in-trap formation of molecular ions in the actinide mass range at CERN-ISOLDE, Nucl. Instrum. Methods Phys. Res. Sect. B **541**, 375 (2023).

[20] E. Mané, J. Billowes, K. Blaum, P. Campbell, B. Cheal, P. Delahaye, K. T. Flanagan, D. H. Forest, H. Franberg, C. Geppert, T. Giles, A. Jokinen, M. Kowalska, R. Neugart, G. Neyens, W. Nörtershäuser, I. Podadera, G. Tungate, P. Vingerhoets, and D. T. Yordanov, An ion cooler-buncher for high-sensitivity collinear laser spectroscopy at ISOLDE, Eur. Phys. J. A **42**, 503 (2009).

[21] M. Doppelbauer, S. C. Wright, S. Hofsäss, B. G. Sartakov, G. Meijer, and S. Truppe, Hyperfine-resolved optical spectroscopy of the $A\,^2\Pi \leftarrow X\,^2\Sigma^+$ transition in MgF, J. Chem. Phys. **156**, 134301 (2022).

[22] T. E. Wall, J. F. Kanem, J. J. Hudson, B. E. Sauer, D. Cho, M. G. Boshier, E. A. Hinds, and M. R. Tarbutt, Lifetime of the $A(v' = 0)$ state and Franck-Condon factor of the $A{-}X$ (0-0) transition of CaF measured by the saturation of laser-induced fluorescence, Phys. Rev. A **78**, 062509 (2008).

[23] L. A. Kaledin, J. C. Bloch, M. C. McCarthy, and R. W. Field, Analysis and deperturbation of the $A\,^2\Pi$ and $B\,^2\Sigma^+$ states of CaF, J. Mol. Spectrosc. **197**, 289 (1999).

[24] P. J. Dagdigian, H. W. Cruse, and R. N. Zare, Radiative lifetimes of the alkaline earth monohalides, J. Chem. Phys. **60**, 2330 (1974).

[25] Y. Hao, L. F. Pašteka, L. Visscher, P. Aggarwal, H. L. Bethlem, A. Boeschoten, A. Borschevsky, M. Denis, K. Esajas, S. Hoekstra, K. Jungmann, V. R. Marshall, T. B. Meijknecht, M. C. Mooij, R. G. Timmermans, A. Touwen, W. Ubachs, L. Willmann, Y. Yin, and A. Zapara, High accuracy theoretical investigations of CaF, SrF, and BaF and implications for laser-cooling, J. Chem. Phys. **151**, 034302 (2019).

[26] P. Aggarwal, V. R. Marshall, H. L. Bethlem, A. Boeschoten, A. Borschevsky, M. Denis, K. Esajas, Y. Hao, S. Hoekstra, K. Jungmann, T. B. Meijknecht, M. C. Mooij, R. G. E. Timmermans, A. Touwen, W. Ubachs, S. M. Vermeulen, L. Willmann, Y. Yin, and A. Zapara (NL-eEDM Collaboration), Lifetime measurements of the $A\,^2\Pi_{1/2}$ and $A\,^2\Pi_{3/2}$ states in BaF, Phys. Rev. A **100**, 052503 (2019).

[27] R. F. Barrow, A. Bernard, C. Effantin, J. D'Incan, G. Fabre, A. El Hachimi, R. Stringat, and J. Vergès, The metastable $A'\,^2\Delta$ state of BaF, Chem. Phys. Lett. **147**, 535 (1988).

[28] X. Zhuang, A. Le, T. C. Steimle, N. E. Bulleid, I. J. Smallman, R. J. Hendricks, S. M. Skoff, J. J. Hudson, B. E. Sauer, E. A. Hinds, and M. R. Tarbutt, Franck-Condon factors and radiative lifetime of the $A\,^2\Pi_{1/2}{-}X\,^2\Sigma^+$ transition of ytterbium monofluoride, YbF, Phys. Chem. Chem. Phys. **13**, 19013 (2011).

[29] T. D. Persinger, J. Han, A. T. Le, T. C. Steimle, and M. C. Heaven, Direct observation of the Yb$(4f^{13}6s^2)$F states and accurate determination of the YbF ionization energy, Phys. Rev. A **106**, 062804 (2022).

[30] S. M. Udrescu, S. G. Wilkins, A. A. Breier, M. Athanasakis-Kaklamanakis, R. F. Garcia Ruiz, M. Au, I. Belošević, R. Berger, M. L. Bissell, C. L. Binnersley, A. J. Brinson, K. Chrysalidis, T. E. Cocolios, R. P. de Groote, A. Dorne, K. T. Flanagan, S. Franchoo, K. Gaul, S. Geldhof, T. F. Giesen *et al.*, Precision spectroscopy and laser-cooling scheme of a radium-containing molecule, Nat. Phys. **20**, 202 (2024).

[31] N. J. Fitch and M. R. Tarbutt, Laser-cooled molecules, in *Advances in Atomic, Molecular, and Optical Physics*, edited by L. F. Dimauro, H. Perrin, and S. F. Yelin (Academic Press, New York, 2021), Vol. 70, Chap. 3, pp. 157–262.

[32] S. Truppe, H. J. Williams, M. Hambach, L. Caldwell, N. J. Fitch, E. A. Hinds, B. E. Sauer, and M. R. Tarbutt, Molecules cooled below the Doppler limit, Nat. Phys. **13**, 1173 (2017).

[33] S. Hofsäss, M. Doppelbauer, S. C. Wright, S. Kray, B. G. Sartakov, J. Pérez-Ríos, G. Meijer, and S. Truppe, Optical cycling of AlF molecules, New J. Phys. **23**, 075001 (2021).

[34] S. C. Wright, M. Doppelbauer, S. Hofsäss, H. Christian Schewe, B. Sartakov, G. Meijer, and S. Truppe, Cryogenic buffer gas beams of AlF, CaF, MgF, YbF, Al, Ca, Yb and NO – A comparison, Mol. Phys. **121**, e2146541 (2023).

[35] N. R. Hutzler, M. F. Parsons, Y. V. Gurevich, P. W. Hess, E. Petrik, B. Spaun, A. C. Vutha, D. DeMille, G. Gabrielse, and J. M. Doyle, A cryogenic beam of refractory, chemically reactive molecules with expansion cooling, Phys. Chem. Chem. Phys. **13**, 18976 (2011).

[36] T. A. Isaev, A. V. Zaitsevskii, and E. Eliav, Laser-coolable polyatomic molecules with heavy nuclei, J. Phys. B: At. Mol. Opt. Phys. **50**, 225101 (2017).

[37] N. J. Fitch, J. Lim, E. A. Hinds, B. E. Sauer, and M. R. Tarbutt, Methods for measuring the electron's electric dipole moment using ultracold YbF molecules, Quantum Sci. Technol. **6**, 014006 (2021).